

# A Proposal of a Hamming Distance Detector with a Neuron CMOS A/D Converter

Makoto Urakami, Masaaki Fukuhara, and Masahiro Yoshida

**Abstract**—In this paper, we propose a new Hamming distance detector using a neuron CMOS A/D converter with two output terminals. The detector outputs the signals which are corresponding to the Hamming distance between two input data immediately. The FPD method is applied to design the ratio of each input capacitance of the proposed detector. To verify the behavior of the proposed detector, the computer simulations were carried out by LTspice.

**Index Terms**—A/D converter, hamming distance detector, neuron MOS.

## I. INTRODUCTION

The similarity of data is important in the fields of pattern matching and data comparison [1]. Hamming distance is one of the measures of the similarity. In the previous studies, the Hamming distance detectors of [2] and [3] determine whether the Hamming distance  $D_H$  between two input data is within a certain range or not by using threshold logic. These detectors have needed many reference signals and clock cycles.

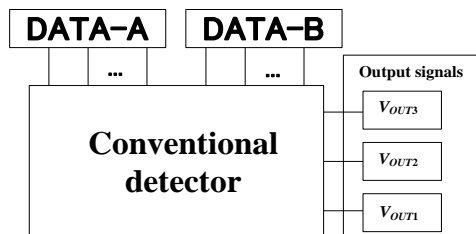


Fig. 1. Block diagram of conventional detector.

TABLE I: THE RELATIONSHIPS OF HAMMING DISTANCE AND OUTPUT SIGNALS OF CONVENTIONAL DETECTOR

Hamming distance $D_H$	$V_{OUT1}$	$V_{OUT2}$	$V_{OUT3}$
0	0	0	0
1	0	0	1
2	0	1	1
More than 3	1	1	1

The other conventional detector determines the Hamming distance  $D_H$  between two input data with no reference signals immediately [4]. The block diagram of the conventional detector is shown in Fig. 1. The detector accepts DATA-A and DATA-B in parallel, and outputs 3-bit signals ( $V_{OUT1}$ ,  $V_{OUT2}$  and  $V_{OUT3}$ ) corresponding to the  $D_H$  between DATA-A and DATA-B as shown in Table I. The detector has required three output terminals, because it outputs 3-bit signals.

In this study, a new Hamming distance detector with a

neuron CMOS A/D converter to reduce the number of output terminals is proposed. The block diagram of the proposed detector is shown in Fig. 2. The detector immediately determines the Hamming distance  $D_H$  between DATA-A and DATA-B with no reference signals and two output terminals. The relationships of  $D_H$  and 2-bit output signals ( $V_{OUT1}$  and  $V_{OUT2}$ ) are shown in Table II. This detector separates the Hamming distance  $D_H$  into four states with employing only two output terminals instead of three output terminals.

The proposed detector is designed by using the FPD. FPD is a method to design the ratio of input capacitances in neuron CMOS circuit graphically. To verify the characteristics of the proposed detector, the computer simulations were carried out by LTspice.

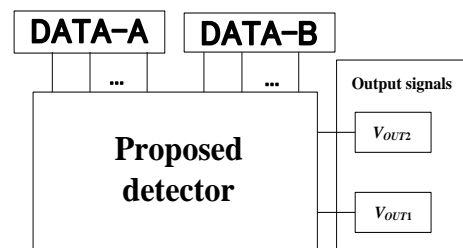


Fig. 2. Block diagram of proposed detector.

TABLE II: THE RELATIONSHIPS OF HAMMING DISTANCE AND OUTPUT SIGNALS OF PROPOSED DETECTOR

Hamming distance $D_H$	$V_{OUT1}$	$V_{OUT2}$
0	1	1
1	1	0
2	0	1
More than 3	0	0

## II. NEURON CMOS INVERTER

The proposed detector employs neuron CMOS inverters as an A/D converter. The construction of the neuron CMOS inverter is shown in Fig. 3. The neuron CMOS inverter consists of a nMOS, a pMOS, capacitors  $C_i$  ( $i=1, 2, \dots, n$ ) and an ordinary CMOS inverter [5]. As shown in Fig. 3, the gate which is connected to the nMOS and pMOS is called floating gate.  $C_i$  ( $i=1, 2, \dots, n$ ) represent the capacitances between the each input gate and the floating gate.

In the Fig. 3,  $V_i$  ( $i=1, 2, \dots, n$ ) is the voltage applying the each input gate,  $\Phi_F$  is the potential of the floating gate,  $V_{OUT}$  is the output voltage and  $V_{DD}$  is the power supply voltage.

$\Phi_F$  is determined by the capacitances  $C_i$  ( $i=1, 2, \dots, n$ ) and the voltages  $V_i$  ( $i=1, 2, \dots, n$ ) as shown by

$$\Phi_F = \frac{\sum_{i=1}^n C_i V_i}{\sum_{i=1}^n C_i} \quad (1)$$

Manuscript received July 9, 2014; revised September 11, 2014.

The authors are with the Tokai University, Tokyo Japan (e-mail: 4bjnm006@mail.tokai-u.jp, fukuhara@tokai.ac.jp, yoshida@tokai.ac.jp).

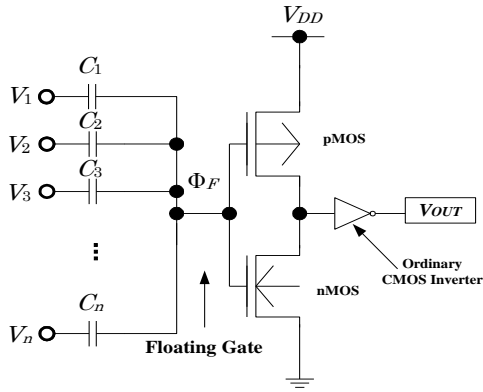


Fig. 3. Schematic diagram of neuron CMOS inverter.

The electrical charge of the floating gate is taken 0 and the capacitance between the substrate and the floating gate is ignored.

Operating states of the neuron CMOS inverter are determined by the relationships of the floating gate potential  $\Phi_F$  and the inversion threshold voltage  $V_{INV}$  as seen from the floating gate. If  $\Phi_F$  is less than  $V_{INV}$ ,  $V_{OUT}$  becomes 0(V). If  $\Phi_F$  is more than  $V_{INV}$ ,  $V_{OUT}$  becomes  $V_{DD}$ .

### III. PROPOSED DETECTOR CONFIGURATION AND DESIGN METHOD

The schematic diagram of the proposed detector is shown in Fig. 4. The detector consists of an XOR array, a D/A converter and an A/D converter using two neuron CMOS inverters (Neuron CMOS1 and Neuron CMOS2). The XOR array is composed of  $n$  two-input XOR gates. The D/A converter has  $M_{N0}$ ,  $M_{P0}$ , and  $M_{Nb}(i=1, 2, \dots, n)$ , the Neuron CMOS1 has  $M_{N1}$ ,  $M_{P1}$ ,  $C_{1,i}(i=1, 2, 3)$  and an ordinary CMOS inverter, and the Neuron CMOS2 has  $M_{N2}$ ,  $M_{P2}$ ,  $C_{2,i}(i=1, 2, 3, 4)$  and an ordinary CMOS inverter.

In the figure,  $A_i(i=1, 2, \dots, n)$  is a bit  $i$  of DATA-A,  $B_i(i=1, 2, \dots, n)$  is a bit  $i$  of DATA-B,  $M_{Ni}(i=0, 1, 2)$  and  $M_{Nbi}(i=1, 2, \dots, n)$  are the nMOS transistor,  $M_{Pi}(i=0, 1, 2)$  are the pMOS transistor,  $C_{1,i}(i=1, 2, 3)$  and  $C_{2,i}(i=1, 2, 3, 4)$  are the capacitance of each input gate of each neuron CMOS inverter,  $V_{ML}$  is the voltage of match line,  $V_{OUT1}$  and  $V_{OUT2}$  are the output voltages,  $\overline{V_{OUT1}}$  is the input voltage of the ordinary CMOS inverter of the Neuron CMOS1 and  $V_{DD}$  is the power supply voltage.

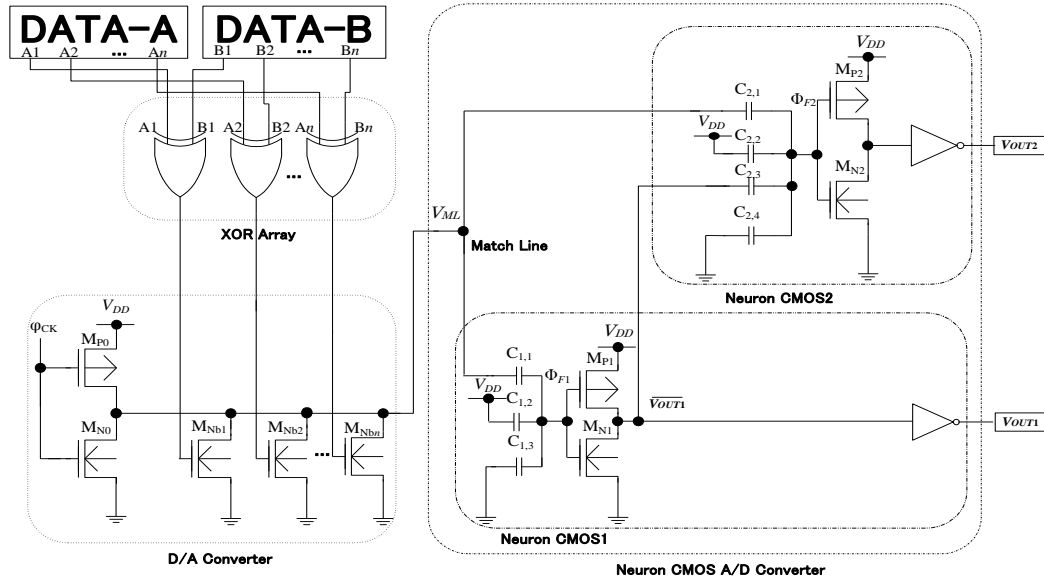


Fig. 4. Schematic diagram of a Hamming distance detector with a neuron CMOS A/D convert.

TABLE III: DEVICE PARAMETERS

	nMOS	pMOS	Unit
Threshold voltage	0.5	-0.8	V
Gate thickness	760	760	Å
Carrier mobility	421	159	cm <sup>2</sup> /Vs

TABLE IV: DIMENSIONS OF MOS TRANSISTORS

Transistor name	W(μm)	L(μm)
MP0	4.5	0.5
MN0, MNb1, MNb2, MNb3	1.0	0.5
MN1, MN2	1.0	0.5
MP1, MP2	4.35	0.5

When the clock signal  $\phi_{CK}$  is low level, the detector operates the Hamming distance detecting operation. When  $\phi_{CK}$  is high level, the detector operates the Reset operation.

At first, the two input data (DATA-A and DATA-B) of bit length  $n$  are applied to the XOR array. Each XOR determines whether the each bit is exact match or inexact match. If  $A_i(i=1, 2, \dots, n)$  equals  $B_i(i=1, 2, \dots, n)$ , XOR outputs 0(V). If  $A_i(i=1, 2, \dots, n)$  and  $B_i(i=1, 2, \dots, n)$  are not equal, XOR outputs  $V_{DD}$ . In the detector, the number of inexact match bit is called Hamming distance  $D_H$ .

In the D/A converter,  $V_{ML}$  is determined corresponding to Hamming distance  $D_H$ . The relationships between  $D_H$  and  $V_{ML}$  which are obtained by the simulations are shown in Fig. 5. To analyze  $V_{ML}$ , computer simulations were carried out by LTspice with 0.35(μm) rules of TSMC. The device parameters are shown in Table III. The dimensions of the MOS transistors are shown in Table IV. Channel lengths L of all MOS transistors are constant at 0.5(μm).  $V_{DD}$  is 3.3(V).

In this paper, we design the ratio of the capacitance of the

each input gate of the neuron CMOS inverters when  $n$  equals 3 as an example by FPD (Floating gate Potential Diagram) [5]. If the Hamming distance  $D_H$  equals 0, then all  $M_{Nbi}$  ( $i=1, 2, \dots, n$ ) are off. Therefore  $V_{ML}$  is  $V_{DD}$  when  $\phi_{CK}$  is low level.  $V_{ML}$  decreases with increasing of the  $D_H$  if  $\phi_{CK}$  is low level as shown in Fig.5. In the simulations,  $V_{ML}$  is 2.48(V) when  $D_H$  equals 1, 1.15(V) when  $D_H$  equals 2 and 0.68(V) when  $D_H$  equals 3.

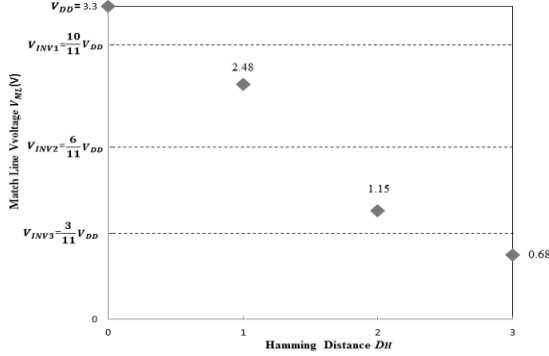


Fig. 5 Relationships between Hamming distance  $D_H$  and match line voltage  $V_{ML}$

In this paper, noise margin is defined as a voltage width between the inversion threshold voltage  $V_{INV}$  of neuron CMOS inverter and  $V_{ML}$  of each distance. To make noise margin larger,  $V_{INV}$  is determined to the middle of  $V_{ML}$  in each distance. In the Fig. 5, each inversion threshold voltage  $V_{INVi}$  ( $i=1, 2, 3$ ) are shown in the dotted line. From the figure,  $V_{INV1}$  is  $\frac{10}{11} V_{DD}$ ,  $V_{INV2}$  is  $\frac{6}{11} V_{DD}$  and  $V_{INV3}$  is  $\frac{3}{11} V_{DD}$ .

In the A/D converter, the output signals of Neuron CMOS1  $V_{OUT1}$  and  $V_{OUT1}$  are determined corresponding to  $V_{ML}$ . The output signal of Neuron CMOS2  $V_{OUT2}$  is determined corresponding to  $V_{ML}$  and  $V_{OUT1}$ . The inversion threshold voltage of Neuron CMOS1 is  $V_{INV2}$ . The inversion threshold voltages of Neuron CMOS2 are  $V_{INV1}$ ,  $V_{INV2}$  and  $V_{INV3}$ .

The FPD of Neuron CMOS1 represents the relationships of floating gate potential  $\Phi_{F1}$ ,  $V_{ML}$  and capacitances  $C_{1,i}$  ( $i=1, 2, 3$ ) between the each input gate and the floating gate as shown in Fig. 6.

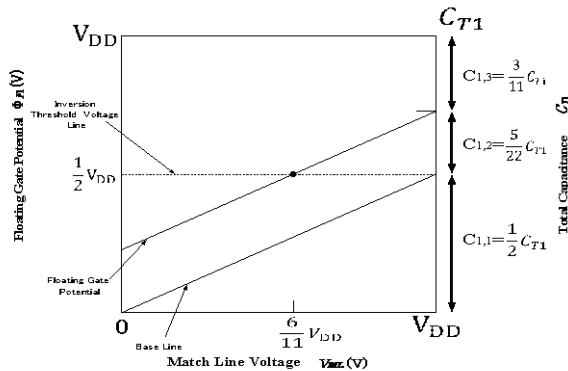


Fig. 6. FPD of Neuron CMOS1.

A vertical axis of left of Fig. 6 is the potential of floating gate  $\Phi_{F1}$  of the Neuron CMOS1, a vertical axis of right is the total capacitance  $C_{T1}$  of each input gate of the Neuron CMOS1, and abscissa is  $V_{ML}$ .  $C_{T1}$  is the total capacitance of  $C_{1,i}$  ( $i=1, 2, 3$ ). We assumed that the inversion threshold voltage as seen from the floating gate is  $\frac{1}{2} V_{DD}$ , and the

inversion threshold voltage line is drawn in the FPD. Then the base line which is the potential of the floating gate when  $V_{ML}$  is varied from 0(V) to  $V_{DD}$  and the other control voltages are 0(V) is drawn. Based on the inversion threshold voltage  $V_{INV2}$  of the Neuron CMOS1, the potential  $\Phi_{F1}$  of the floating gate corresponding to the  $V_{ML}$  is drawn. The ratio of each capacitance is indicated graphically as a split ratio of the vertical axis of right. Hence, the ratio of the capacitances of the Neuron CMOS1 is  $C_{1,1} : C_{1,2} : C_{1,3} = 11 : 5 : 6$  as shown in Fig. 6.

The FPD of the Neuron CMOS2 is shown in Fig. 7. In the Fig. 7, a vertical axis of left is the potential  $\Phi_{F2}$  of the floating gate of Neuron CMOS2, a vertical axis of right is the total capacitance  $C_{T2}$  of each input gate of the Neuron CMOS2 and abscissa is  $V_{ML}$ .  $C_{T2}$  is the total capacitance of  $C_{2,i}$  ( $i=1, 2, 3, 4$ ). Based on the inversion threshold voltages  $V_{INV1}$ ,  $V_{INV2}$  and  $V_{INV3}$  of the Neuron CMOS2, the potential  $\Phi_{F2}$  corresponding to the  $V_{ML}$  is drawn in Fig. 7. From the figure, the ratio of the capacitances of the Neuron CMOS2 is  $C_{2,1} : C_{2,2} : C_{2,3} : C_{2,4} = 11 : 1 : 7 : 3$ .

We designed the capacitances of the input gates as shown in Table V from the FPDs.

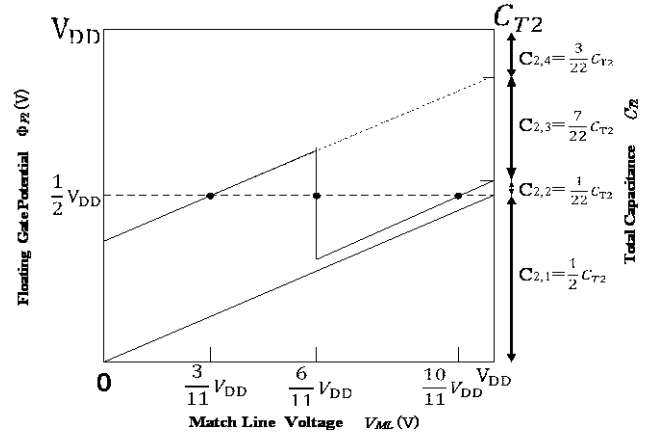


Fig. 7. FPD of neuron CMOS2.

TABLE V: CAPACITANCES OF EACH INPUT GATE OF NEURON CMOS1 AND NEURON CMOS2

Capacitor name	C(ff)
$C_{1,1}$	220
$C_{1,2}$	100
$C_{1,3}$	120
$C_{2,1}$	220
$C_{2,2}$	20
$C_{2,3}$	140
$C_{2,4}$	60

#### IV. SIMULATION WAVEFORMS

To verify the proposed detector, the computer simulations were carried out by LTspice.

Simulation waveforms are shown in Fig. 8. In this simulation,  $V_{DD}$  is taken 3.3(V), 0 of the Table II is taken 0(V) and 1 of the Table II is taken  $V_{DD}$ . Fig. 8(a) is the waveform of clock  $\phi_{CK}$ . The operating states are divided by 2 states. These are reset operation when  $\phi_{CK}$  is 3.3 (V), and Hamming distance detecting operation when  $\phi_{CK}$  is 0(V). Fig. 8(b) is the waveforms when the Hamming distance  $D_H$  equals 0. As shown in Fig. 8 (b),  $V_{OUT1}$  outputs  $V_{DD}$  and  $V_{OUT2}$  outputs  $V_{DD}$  during the Hamming distance detecting operation. Fig. 8(c) is the waveforms when the  $D_H$  equals 1. As shown in Fig. 8(c),  $V_{OUT1}$  outputs  $V_{DD}$  and  $V_{OUT2}$  outputs 0(V) during the

Hamming distance detecting operation. Fig. 8 (d) is the waveforms when the Hamming distance  $D_H$  equals 2. As shown in Fig. 8(d),  $V_{OUT1}$  outputs 0(V) and  $V_{OUT2}$  outputs  $V_{DD}$  during the Hamming distance detecting operation. Fig. 8(e) is the waveforms when the  $D_H$  equals 3. As shown in Fig. 8(e),  $V_{OUT1}$  outputs 0(V) and  $V_{OUT2}$  outputs 0(V) during the Hamming distance detecting operation.

From these waveforms, this detector behaves properly as shown in Table II.

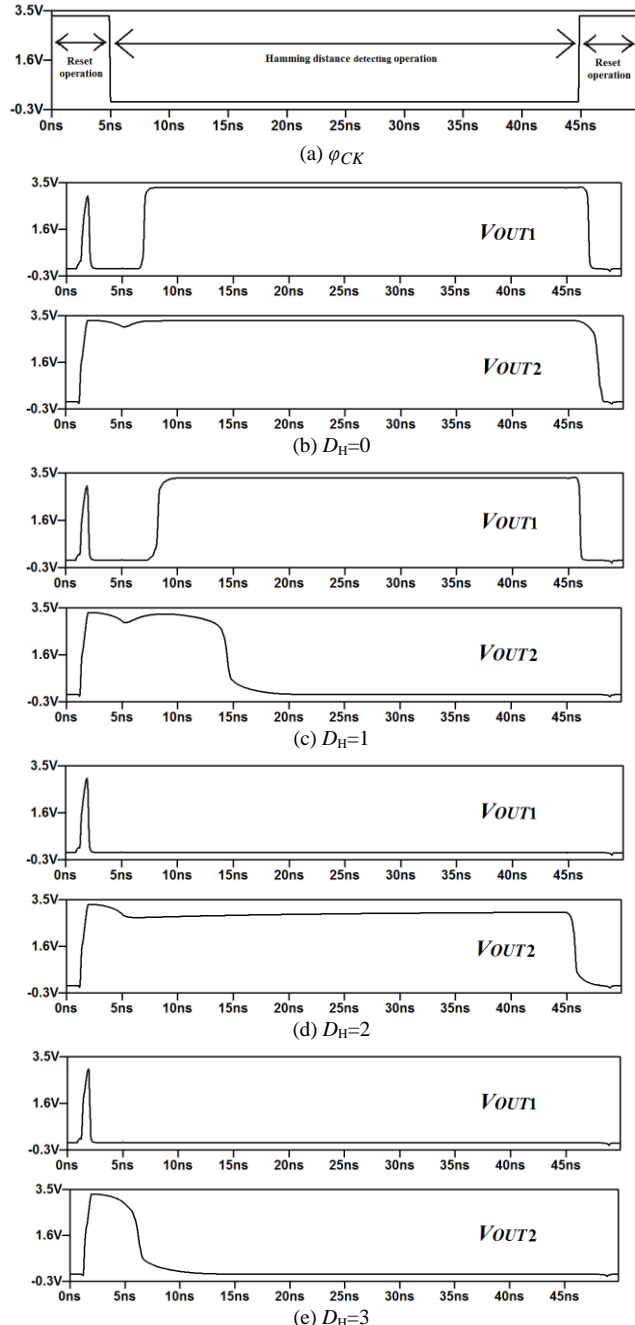


Fig. 8. Simulation waveforms.

## V. CONCLUSION

In this paper, we proposed the Hamming distance detector using a neuron CMOS A/D converter with 2 output terminals. This detector immediately detects Hamming distance between 2 input data. We verified that the proposed detector properly behaved by using LTspice. As shown in the simulation results, the detector has a delay from starting

Hamming distance detecting operation to output the distance particularly in the circuit outputs 0(V). It is considered that the floating gate potential behaves around the inversion threshold voltage. One of the solutions of delay is using clock neuron CMOS inverter [6].

We consider that the proposed detector can be applied for pattern matching of antivirus system or dictionary search. In the future, the proposed detector may be applied to CAM.

## ACKNOWLEDGMENT

The authors wish to thank to Mr. Yoshiki Sato for giving the advice of the proposed detector.

## REFERENCES

- [1] H. J. Mattausch, T. Gyohten, Y. Soda, and T. Koide, "Compact associative-memory architecture with fully-parallel search capability for the minimum hamming distance," *IEEE Journal of Solid-State Circuits*, vol. 37, no. 2, pp. 218-227, 2002.
- [2] H. Yamaoka and K. Asada, "A threshold logic-based high-speed hamming distance detector and its evaluation," *Technical Report of IEICE*, pp. 37-42, 2001.
- [3] M. Fukuhara and M. Yoshida, "Proposal of a hamming distance detector using neuron MOS transistors," *Institute of Electrical Engineers of Japan Trans., A publication of Electronics, Information and System Society*, vol. 124, no. 10, pp. 2044-2050, Oct. 2004.
- [4] W. R. Daasch and J. Lee, "A word/bit parallel inexact match content addressable memory," in *Proc. IEEE International ASIC Conference and Exhibit*, pp. 25-28, 1994.
- [5] T. Shibata and T. Ohmi, "Neuron MOS binary-logic integrated circuits-part I: Design fundamentals and soft- hardware-logic circuit implementation," *IEEE Trans. Electron Devices*, vol. 40, no. 3, pp. 570-576, Mar. 1993.
- [6] H. Takahashi, M. Fukuhara, and M. Yoshida, "Configuration of a low power carom using clocked neuron cmos inverters and its operating characteristics," *The School of Information and Telecommunication Eng., Tokai Univ., Tokyo, Japan*, vol. 6, no. 2, pp. 9-14, 2013.



**Makoto Urakami** was born in Kobe, Japan on March 19, 1992.

He received B.E. degree in Dept. Embedded Technology from Tokai University, Tokyo, Japan in 2014. Since 2014, he is a master student in Tokai University Graduate School of Information and Telecommunication Engineering. His current interests include low power CMOS LSI and neuron MOS LSI.



**Masaaki Fukuhara** was born in Yokohama, Japan on December 20, 1979.

He received B.E., M.E. and Dr. Eng. degrees in Dept. of Electrical Eng. from Tokai University, Hiratsuka, Japan in 2002, 2004, and 2007 respectively. Since 2013, he is an assistant professor of Dept. of Embedded Technology, Tokai University. His current research interests include CAM LSI's, low power CMOS LSI's and charge-pump circuits. Mr. Fukuhara is a member of IEICE.



**Masahiro Yoshida** was born in Fukushima, Japan on December 16, 1951.

He received B.E., M.E. and Dr. Eng. degrees in Dept. of Electrical Eng. from Tokai University, Hiratsuka, Japan in 1976, 1978, and 1990 respectively. He joined Tokai University as an assistant in 1978 and promoted to a professor of same university in 1995. Since 2008, he is a professor of Dept. of Embedded Technology, Tokai University. "A DC-DC Converter Using Chopper Comparators for LTPS-TFT" (Tokyo: IEICE, 2011), "New Bias Voltage Generators for TFT-LCD's Drivers" (Tokyo: IEICE, 2000) His current research interests include CAM LSI's, low power CMOS LSI's and charge-pump circuits. Mr. Yoshida is a member of IEICE.